ELSEVIER

Chemical Engineering Journal 137 (2008) 422–427

Chemical Engineering Journal

www.elsevier.com/locate/cej

Effect of bubble contamination on gas–liquid mass transfer coefficient on CO_2 absorption in amine solutions

Rocío Maceiras [a,*], Sebastião S. Alves [b], M. Ángeles Cancela [a], Estrella Álvarez [a]

[a] *Chemical Engineering Department, E.T.S.E.I., Rúa Maxwell s/n, 36310 Vigo, Spain*

[b] *Institute for Biotechnology and Bioengineering (IBB), Centre for Biological and Chemical Engineering, Instituto Superior Técnico, Av. Rovisco Pais, 1049-001 Lisboa, Portugal*

Received 16 October 2006; received in revised form 18 April 2007; accepted 24 April 2007

Abstract

An electrochemical method was used to follow CO_2 absorption both in water and in alkanolamine solutions in a bubble column (∼1 m tall). This method allows the determination of local mass transfer coefficients along the column. No special care was taken in avoiding trace contaminants. It was found that bubbles contaminate mostly at the gas distributor. Gas–liquid mass transfer coefficient decreases as bubbles rise along the column, taking values closer to those expected for clean bubbles with a mobile surface at the bottom of the column, and values closer to those expected for rigid bubbles, at the top of the column. If this is quantitatively interpreted within the framework of the stagnant cap model, it may be concluded that this decrease is mainly due to bubble shrinkage, which leads to a greater fraction of bubble area being covered by the stagnant cap. Compared with this effect, the effect of further acquisition of contaminant molecules by the bubbles is negligible. The above conclusions can be drawn both for absorption with chemical reaction in amine solutions and for pure absorption of CO_2 in tap water, although in this case the shrinkage effect is less pronounced.

Keywords: Bubble column; Absorption; Gas–liquid mass transfer coefficients; Stagnant cap; DEA; MDEA

1. Introduction

Bubble column reactors are used in a variety of industries, such as in fine chemical production, oxidation and hydrogenation reactions, in fermentation, etc. Their main advantages are easy construction, high gas–liquid interfacial area, good mass transfer rate between gas and liquid phase and large liquid holdup [1].

Characteristic design parameters for this device are gas–liquid interfacial area, mass transfer coefficients, flow regime, bubble size distribution and bubble coalescence. In gas–liquid processes, the volumetric mass transfer coefficient, k_La, is a key parameter to estimate reactor performance.

While most studies determine k_La as a global parameter, it is recognized [2,3] that this is insufficient to understand the gas–liquid mass transfer mechanism. Thus some authors have separately determined k_L and a values in bubble columns [4,5,6].

It is generally recognized that gas–liquid mass transfer between a bubble and surrounding liquid is highly dependent upon overall surface mobility, which is affected by contamination by surfactants. Upper values of mass transfer coefficient, k_L, occur for a bubble with a totally mobile surface, for which its value may be predicted using Higbie's equation [7]:

$$k_L^{\text{mobile}} = 1.13\sqrt{\frac{u}{d}}D^{1/2} \quad (1)$$

where d is the bubble diameter, u the bubble-liquid relative velocity (slip velocity) and D is the diffusivity.

Lower values of mass transfer coefficient occur for a bubble with a totally rigid surface, for which its value may be predicted using an equation proposed by Frössling [8] from laminar boundary layer theory:

$$k_L^{\text{rigid}} = c\sqrt{\frac{u}{d}}D^{2/3}\nu^{-1/6} \quad (2)$$

where $c \approx 0.6$ and ν is the kinematic viscosity of the liquid.

A conceptual model that has been used to interpret data and theorize about gas–liquid mass transfer to bubbles is the stagnant

* Corresponding author. Tel.: +34 986 812 213; fax: +34 986 812 201.
E-mail address: rmaceiras@uvigo.es (R. Maceiras).

1385-8947/$ – see front matter © 2007 Elsevier B.V. All rights reserved.
doi:10.1016/j.cej.2007.04.036

Nomenclature

a	interfacial area (m^{-1})
A	total bubble area (m^2)
A_{cap}	area of the stagnant cap surface (m^2)
C_A^*	solubility of CO_2 (kmol m^{-3})
C_{Bo}	initial concentration of alkanolamine (kmol m^{-3})
d	bubble diameter (m)
d_{32}	Sauter mean diameter (m)
D	diffusion coefficient ($m^2\ s^{-1}$)
D_A	diffusion coefficient of CO_2 in the aqueous alkanolamine solution ($m^2\ s^{-1}$)
e	ellipsoid minor axis (m)
E	ellipsoid major axis (m)
He	Henry constant (atm m^3/kmol)
k	second-order rate coefficient (m^3 (kmol s)$^{-1}$)
k_L	individual mass transfer coefficient (m s^{-1})
k_L^*	normalized mass transfer coefficient
k_La	volumetric mass transfer coefficient (s^{-1})
n	number of bubbles
R_A	absorption rate per unit volume (kmol (L s)$^{-1}$)
T	temperature (K)
u	bubble-liquid relative velocity (m s^{-1})

Greek letters

ε	gas holdup
ν	liquid kinematic viscosity ($m^2\ s^{-1}$)

cap model [9,10]. This assumes that surface active contaminant molecules which adsorb at the bubble interface are displaced toward the rear of the bubble forming a cap with immobile surface (the stagnant cap), while the rest of the bubble surface remain mobile. Average k_L for the bubble may be estimated [11,12] using

$$k_L = \frac{k_L^{mobile}(A - A_{cap}) + k_L^{rigid} A_{cap}}{A} \quad (3)$$

In this study mass transfer coefficients are determined in the absorption of CO_2 both into water and into aqueous solutions of alkanolamines. This allows testing the stagnant cap model in a situation of absorption with chemical reaction and comparing it with purely physical absorption.

2. Experimental

2.1. Experimental set-up and procedure

The mass transfer measurements were performed in a square bubble column (1) made of methacrylate, 1.03 m height and 6 cm side length (Fig. 1). For the injection and uniform distribution of the gas phase, a gas sparger, i.e., a porous plate (8) of 4 mm in diameter is installed at the centre of the bottom plate (7). This plate has another two orifices for liquid outlet (5) and for a thermometer (6). There are also three orifices at the top plate: liquid inlet (2), gas outlet (3) and another thermometer (4).

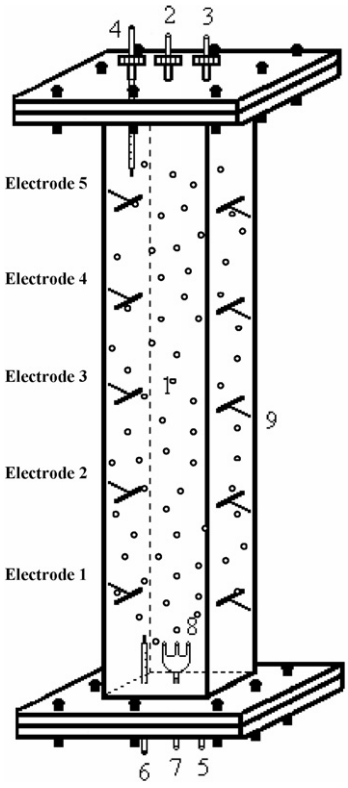

Fig. 1. Schematic figure of the bubble column reactor.

The column has, in two of its internal walls, five pairs of steel electrodes INOX 316 (9) of 1 cm wide and 6 cm length, separated to each other 22 cm. The electrodes are connected to a digital voltmeter to measure the potential between each pair of electrodes every 0.5 s, and a generator which feeds alternating current at 1 kHz.

Each experiment run was started by filling the column with appropriate liquid phase up to 100 cm above the sparger. The feed carbon dioxide was passed through a humidifier at the ambient temperature to prepare the gas phase. The gas flow, before entering the bubble column, was metered by a flow meter and controlled with a flow controller Brooks 0154. The gas flow in the outlet was measured with a soap meter every 1 min.

Mass transfer coefficients can be obtained through conductivity measurements because CO_2 reacts in liquid phase according to the equations:

$$R_2NH + CO_2 \rightarrow HCO_3^- + R_2NH_2^+$$

$$CO_2 + H_2O \rightarrow H_2CO_3$$

$$CO_2 + OH^- \rightarrow HCO_3^-$$

The ionic concentration in solution is thus proportional to the absorbed CO_2 and is measurable using the Debye-Hückel law [13]:

$$\lambda = K\sqrt{C_A} - \lambda_0 \quad (4)$$

Finally, the gas absorption rate was calculated as the slope of the CO_2 concentration versus time. All the details about cali-

Table 1
Kinetic parameter for alkanolamine solutions

T (K)	k_{DEA} ($m^3\ kmol^{-1}\ s^{-1}$)	k_{MDEA} ($m^3\ kmol^{-1}\ s^{-1}$)
293	6.36	2.564
298	9.41	3.622
303	12.80	5.047

bration, data acquisition and analysis techniques are reported in Maceiras et al. [14,15].

In this work only data from electrodes 2 (bottom) and 5 (top) were used, for the following reasons: (i) electrode 1 is too close to the distributor; (ii) data from adjacent electrodes are likely to be significantly affected by liquid mixing; this is not the case between electrodes as widely separated (0.66 m) as 2 and 5 (mixing times of the order of 1 min, whereas measuring time is of the order of 1 s).

Aqueous diethanolamine (DEA) and methyldietanolamine (MDEA) solutions of different concentrations were employed as liquid phase, while the gas phase was carbon dioxide with a different gas flow rate for each run. The amine concentrations were varied between 0 and 1.0 M, and the gas flow rates between 10 and 25 L/h.

2.2. Mass transfer coefficients

The reaction regime between CO_2 and DEA or MDEA solutions is rapid [16–20]. In this case, the rate of absorption of carbon dioxide per unit volume, R_A, is computed from the following expression [15]:

$$R_A = C_A^* \sqrt{(k_L a)^2 + a^2 k C_{Bo} D_A} \quad (5)$$

where $k_L a$ is the volumetric mass transfer coefficient, k the kinetic constant, D_A the diffusion coefficient of CO_2 in the aqueous alkanolamine solution, C_A^* the solubility, C_{Bo} the initial concentration of alkanolamine and a is the interfacial area. The kinetic parameter k was independently determined [14] and the experimental values are shown in Table 1. Values of solubility have been obtained from the literature [21–25] using Henry's Law and are given in Table 2.

Eq. (5) can be rearranged to obtain the volumetric mass transfer coefficient, if the absorption rate and the interfacial area are known:

$$k_L a = \sqrt{\left(\frac{R_A}{C_A^*}\right)^2 - a^2 k C_{Bo} D_A} \quad (6)$$

The individual mass transfer coefficient, k_L, was calculated with the following expression:

$$k_L = \frac{k_L a}{a} \quad (7)$$

2.3. Bubble size

The carbon dioxide bubble dimensions were determined by means of an image digital analysis that involves shooting a film with a high-speed digital video camera (SONY DCR-TRV9E) in order to, subsequently, extract selected snapshots using STUDIO Version 7 software. The images were recorded during 30 s in three different sections of the column until the saturation was reached. Changes in bubble size over the height of the column were determined by recording films at distances of 20, 45 and 85 cm above the sparger.

Table 2
Henry constant for alkanolamine solutions

T (K)	[amine] ($kmol/m^3$)	He_{DEA} ($atm\ m^3/kmol$)	He_{MDEA} ($atm\ m^3/kmol$)
293	0.05	25.6859	25.6575
	0.10	25.7119	25.6575
	0.30	25.8545	25.6575
	1.00	26.8108	25.6575
298	0.05	29.8522	29.8192
	0.10	29.8825	29.8192
	0.30	30.0482	29.8192
	1.00	31.1595	29.8192
303	0.05	34.5226	34.4845
	0.10	34.5576	34.4845
	0.30	34.7493	34.4845
	1.00	36.0344	34.4845

It is important to note that the software and photographic techniques only allow two-dimensional measurements on the bubbles. The observed bubbles have mainly ellipsoidal shapes characterized by the major axis, E, which represents the largest distance between two points on a bubble, and the minor axis, e, which represents the largest length of a line, perpendicular to the major axis, that join two points of the bubble. Both axis were measured using *UTHSCSA Image Tool* software. With this information, the bubble diameter associated with an equivalent diameter of a sphere with the same volume as the ellipsoid was calculated as follows:

$$d = \sqrt[3]{E^2 e} \quad (8)$$

The Sauter mean diameter [1] was used to obtain an adequate average diameter for each experiment:

$$d_{32} = \frac{\sum_i n_i d_i^3}{\sum_i n_i d_i^2} \quad (9)$$

where n_i is the number of bubbles having an equivalent diameter d_i.

The gas–liquid interfacial area is given by

$$a = \frac{6\varepsilon}{d_{32}(1-\varepsilon)} \quad (10)$$

where ε is the gas holdup and d_{32} is the mean Sauter diameter. Gas holdup is calculated from photography at three levels in the column, from bubble number and volume.

3. Results and discussion

Fig. 2 shows k_L values for DEA and MDEA solutions obtained at the bottom of the column (electrode 2) and at the top of the column (electrode 5). Data for water are superim-

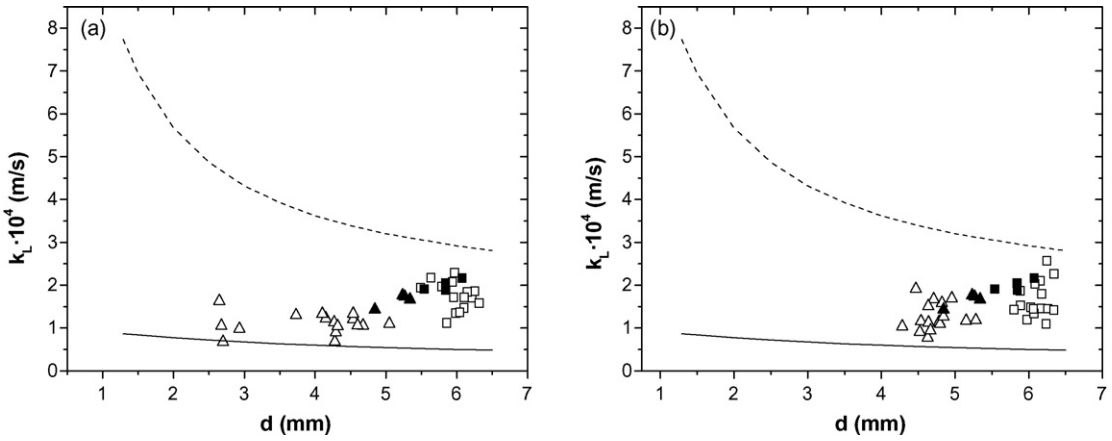

Fig. 2. Effect of bubble diameter on k_L: (a) for DEA and water solutions; (b) for MDEA and water solutions: (■) electrode 2-water, (▲) electrode 5-water, (□) electrode 2-amine solution, and (△) electrode 5-amine solution.

posed in both figures and besides, Higbie's equation Eq. (1) and Frössling equation Eq. (2). Values of k_L are between Higbie and Frössling indicating that the bubbles do not have a totally mobile or totally rigid behaviour.

Despite some dispersion, it is clear that values of k_L approach Higbie more at the bottom of the column (electrode 2), where bubbles are larger, while values of k_L are closer to Frössling at the top of the column (electrode 5), where bubbles are smaller.

This is even clearer if data are plotted in dimensionless form (Fig. 3), as the normalized mass transfer coefficient, k_L^*, calculated with the following expressions:

$$k_L^* = \frac{k_L - k_{L,\text{rigid}}}{k_{L,\text{mobile}} - k_{L,\text{rigid}}} \tag{11}$$

where k_L^* is one if the bubble surface is mobile, it is zero if the bubble is rigid.

The bubble starts almost clean, although there is always some degree of contamination at bubble formation. Then, along its upward path along the column (from electrode 2 to electrode 5), the bubble shrinks and becomes increasingly rigid.

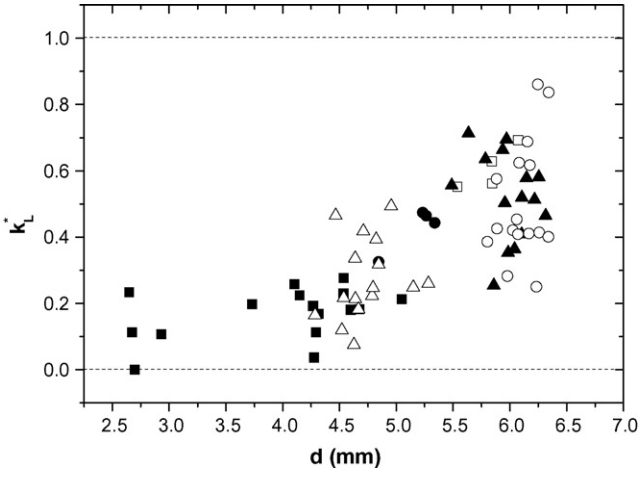

Fig. 3. k_L^* vs. bubble diameter: water: (□) electrode 2, (●) electrode 5; DEA solutions: (▲) electrode 2, (■) electrode 5; MDEA solutions: (◯) electrode 2, (△) electrode 5.

Despite a considerable amount of dispersion, amine solutions and water appear to behave in the same way as regards k_L^*. The major difference in behaviour lies in bubble shrinkage. As expected, bubbles shrink less in water (physical absorption of CO_2) than in the amine solutions. Bubbles shrink the most in solutions of DEA. Apart from that, all points in the k_L^* versus diameter plot follow the same trend line, regardless of solution composition.

It is also clear from the data that bubbles are already considerably contaminated at the bottom of the column, contamination resulting probably from the process of bubble formation. Contamination at this stage has a high degree of dispersion associated to it.

These facts plus the fact that bubbles have a short residence time in the column (∼5 s) suggest the following hypothesis: (i) the bubbles acquire most of the contaminant during formation; (ii) the bubbles become more rigid (as reflected in lowering of k_L^*) due to the increase in the fraction of their area covered by the stagnant cap; (iii) this increase is almost solely due to bubble shrinkage, i.e., the amount of contaminant does not increase significantly, but its average surface concentration increases due to the decrease of bubble surface area (Fig. 4).

The hypothesis can be tested using the experimental data above. Within the framework of the stagnant cap model, the

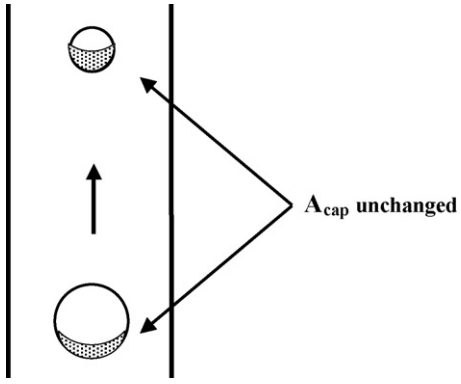

Fig. 4. Stagnant cap.

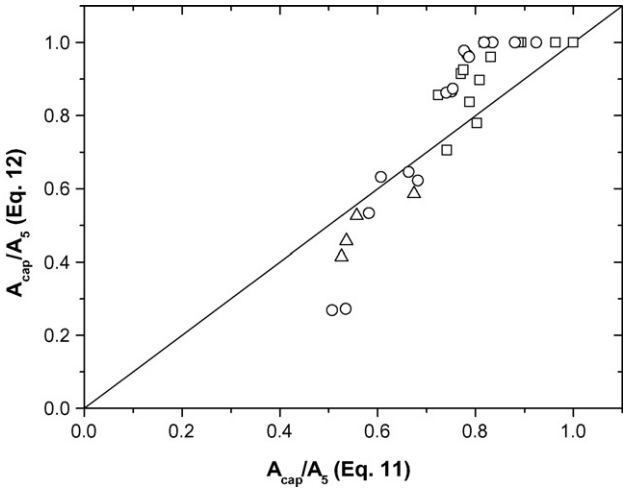

Fig. 5. Comparison between values of A_{cap}/A_5 calculated with eqs. (11) and (12): (□) DEA, (◯) MDEA, and (△) water.

fraction of stagnant cap area A_{cap}/A may be calculated from k_L (Eq. (3)), assuming that the rigid part of the bubble and the mobile part of the bubble each contributes to the mass transfer, the former with a coefficient given by Frössling's equation, the latter a coefficient given by Higbieĭs equation. A_{cap}/A may thus be calculated for positions 2 and 5.

For position 5, on the other hand, there is an alternative, independent way of calculating A_{cap}/A, if the above hypothesis holds, i.e., if no further contaminant is collected by the bubble along its relatively short rising path. In this case $A_{cap,2} = A_{cap,5} = A_{cap}$. Hence

$$\frac{A_{cap}}{A_2} = \frac{A_{cap}}{A_5} \times \frac{A_5}{A_2} = \frac{A_{cap}}{A_5} \times \left(\frac{d_5}{d_2}\right)^2 \quad (12)$$

Fig. 5 presents values of A_{cap}/A_5 for bubbles at the top of the column, as calculated in both ways, i.e., directly from experimental values of k_L through Eq. (11), and in the ordinates as calculated from A_{cap}/A_2 and Eq. (12). Note that when the value calculated through Eq. (12) exceeds one, this means that the initial amount of contaminant is more than enough to cover the bubble, i.e, the stagnant cap covers the bubble. In this case, the value attributed to A_{cap}/A_2 from this calculation is one, since physically A_{cap} cannot be greater than A_2.

Most points are close to the diagonal, which is consistent with the hypothesis made. Points above the line are those corresponding to bubbles for which shrinkage alone should ensure that the stagnant cap fulfils the entire bubble surface. Deviation must be attributed to experimental error. Points below the diagonal correspond to bubbles which end up more rigid (lower k_L) than was expected from shrinkage alone. Only two points are clear in these conditions.

4. Conclusions

For bubbles rising in a relatively shallow bubble column (∼1 m tall), without special care in getting rid of trace contaminants, the following conclusions were drawn:

(i) Bubbles contaminate mostly when they are formed, i.e., at the gas distributor. This process adds a lot of dispersion to experimental results.

(ii) Gas–liquid mass transfer coefficient decreases as the bubble rises along the column. If this is quantitatively interpreted within the framework of the stagnant cap model, it may be concluded that this decrease is mainly due to bubble shrinkage, which leads to a greater fraction of bubble area being covered by the stagnant cap. Compared with this effect, the effect of further acquisition of contaminant molecules by the bubbles is negligible.

(iii) The above conclusions can be drawn both for pure absorption of CO_2 in tap water and for absorption with chemical reaction in amine solutions.

References

[1] Y.T. Shah, B.G. Kelkar, S.P. Godbole, W.D. Deckwer, Design parameters estimations for bubble column reactors, AIChE J. 28 (1982) 353–379.
[2] G. Vázquez, M.A. Cancela, R. Varela, E. Álvarez, J.M. Navaza, Influence of surfactants on absorption of CO_2 in a stirred tank with and without bubbling, Chem. Eng. J. 67 (1997) 131–137.
[3] C. Akosman, R. Orhan, G. Dursun, Effects of liquid property on gas holdup and mass tranfer in co-current downflow contacting column, Chem. Eng. Process. 43 (2004) 503–509.
[4] K. Akita, F. Yoshida, Bubble size, interfacial area, and liquid phase mass transfer coefficients in bubble columns, Indus. Eng. Chem. Process Design Develop. 13 (1) (1974) 84–91.
[5] G. Vázquez, M.A. Cancela, C. Riverol, E. Álvarez, J.M. Navaza, Application of the Danckwerts method in a bubble column. Effects of surfactants on mass transfer coefficient and interfacial area, Chem. Eng. J. 78 (2000) 13–19.
[6] J.M.T. Vasconcelos, J.M.L. Rodrigues, S.C.P. Orvalho, S.S. Alves, R.L. Mendes, A. Reis, Effect of contaminants on mass transfer coefficients in bubble column and airlift contactors, Chem. Eng. Sci. 58 (2003) 1431–1440.
[7] R. Higbie, The rate of absorption of pure gas into a still liquid during short periods of exposure, Trans. Amer. Inst. Chem. Eng. 31 (1935) 365–389.
[8] N. Frössling, Über die verdünstung fallenden tropfen (Evaporation of falling drops), Gerlands Beitage zur Geophysik 52 (1938) 170–216.
[9] J.A. Ramirez, R.H. Davis, Mass transfer to a surfactant-covered bubble or drop, Am. Inst. Chem. Eng. J. 45 (1999) 1355–1358.
[10] F. Takemura, A. Yabe, Rising speed and dissolution rate of a carbon dioxide bubble in slightly contaminated water, J. Fluid Mech. 378 (1999) 319–334.
[11] P. Painmanakul, K. Loubière, G. Hèrbrard, M. Mietton-Peuchot, M. Roustan, Effect of surfactants on liquid-liquid-side mass transfer coefficients, Chem. Eng. Sci. 60 (2005) 6480–6491.
[12] S.S. Alves, S.C.P. Orvalho, J.M.T. Vasconcelos, Effect of bubble contamination on rise velocity and mass transfer, Chem. Eng. Sci. 60 (2005) 1–9.
[13] G. Prentice, Electrochemical Engineering Principles, Prentice-Hall, Inc., New Jersey, 1991.
[14] R. Maceiras, Absorción de dióxido de carbono en disoluciones acuosas de alcanolaminas: Aplicación de Técnicas electroquímicas. PhD Thesis, University of Vigo, Spain, 2006.
[15] R. Maceiras, E. Álvarez, M.A. Cancela, X.R. Nóvoa, Local mass transfer measurements in a bubble column using an electrochemical technique, Chem. Eng. Process, (2007).
[16] G.F. Versteeg, W.P.M. Van Swaaij, On the kinetic between CO_2 and alcanolamines both in aqueous and non-aqueous solutions-I. Primary and secondary amines, Chem. Eng. Sci. 43 (1988) 573–585.
[17] G.F. Versteeg, W.P.M. Van Swaaij, On the kinetic between CO_2 and alcanolamines both in aqueous and non-aqueous solutions-II. Tertiary amines, Chem. Eng. Sci. 43 (1988) 587–591.

[18] R.J. Littel, G.F. Versteeg, W.P.M. Van Swaaij, Kinetics of carbon dioxide with tertiary amines in aqueous solutions, AIChE J. 36 (1990) 1633–1640.
[19] R.J. Littel, G.F. Versteeg, W.P.M. Van Swaaij, Kinetics of CO_2 with primary and secondary amines in aqueous solutions-II, Chem. Eng. Sci. 47 (1992) 2037–2045.
[20] F. Camacho, S. Sánchez, R. Pacheco, R. Maceiras, M.D. La Rubia, A. Sánchez, Absorption of carbon dioxide in solutions of monoethanolamine, diethanolamine and methyldiethanolamine. Comparative analysis and influence of thermal effects, in: Proceedings of the 7th World Congress of Chemical Engineering, 2005.
[21] P.V. Danckwerts, M.M. Sharma, The absorption of carbon dioxide into solutions of alcalis and amines, Chem. Eng. 10 (1966) CE244–CE280.
[22] E. Sada, H. Kumazawa, M.A. Butt, Solubility and diffusivity of gases in aqueous solutions of amines, J. Chem. Eng. Data 23 (1978) 161–163.
[23] C. Blanc, G. Demarais, The reaction rate of CO_2 with diethanolamine, Int. Chem. Eng. 24 (1984) 43–52.
[24] G.F. Versteeg, P.M.M. Blauwhoff, W.P.M. van Swaaij, The effect of diffusivity on gas-liquid mass transfer in stirred vessels. Experiments at atmospheric and elevated pressures, Chem. Eng. Sci. 42 (1987) 1103–1109.
[25] G.F. Versteeg, W.P.M. Van Swaaij, Solubility and diffusivity of acid gases (CO_2, N_2O) in aqueous alkanolamine solutions, J. Chem. Eng. Data 33 (1988) 29–34.